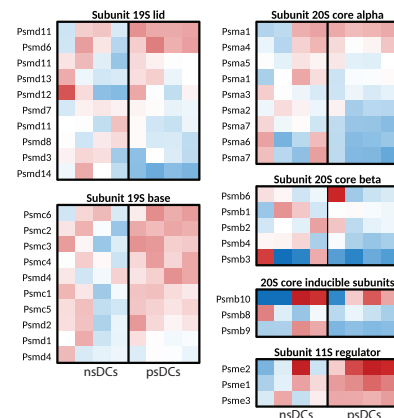
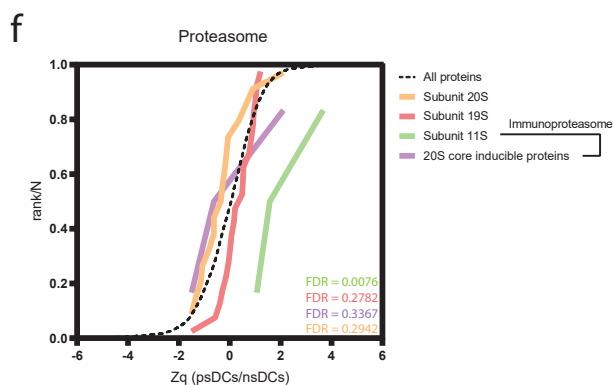
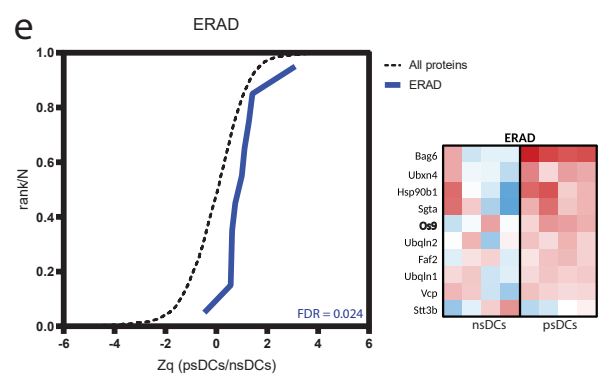
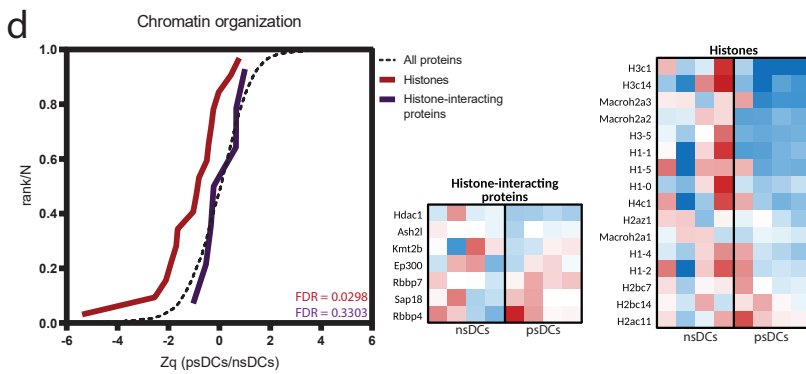
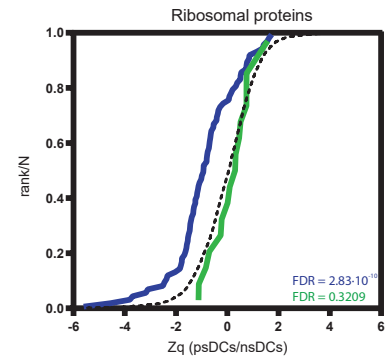
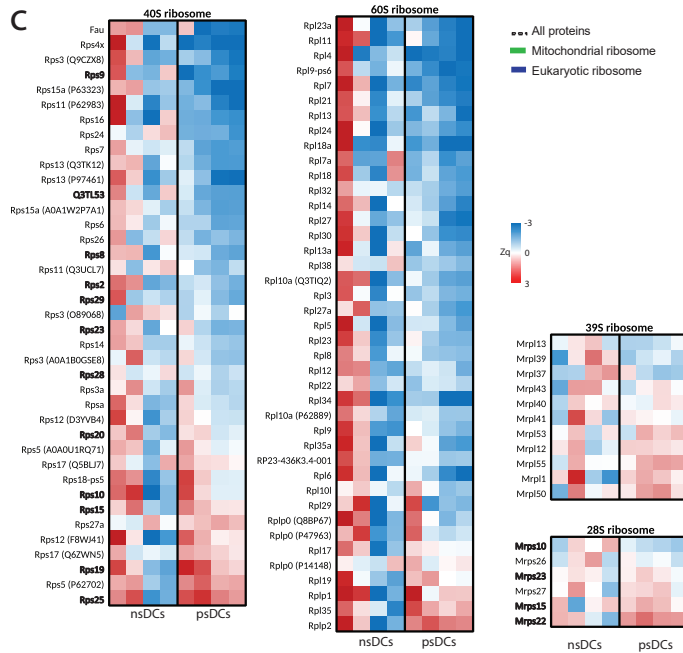
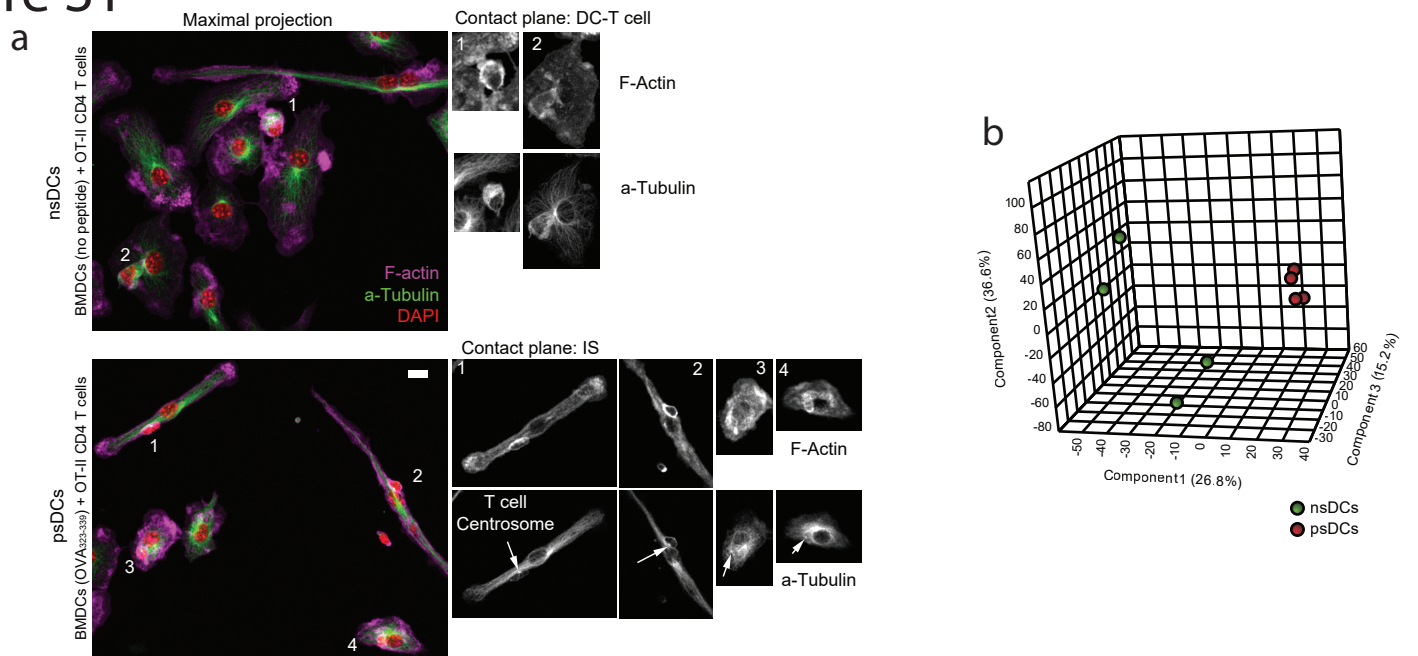


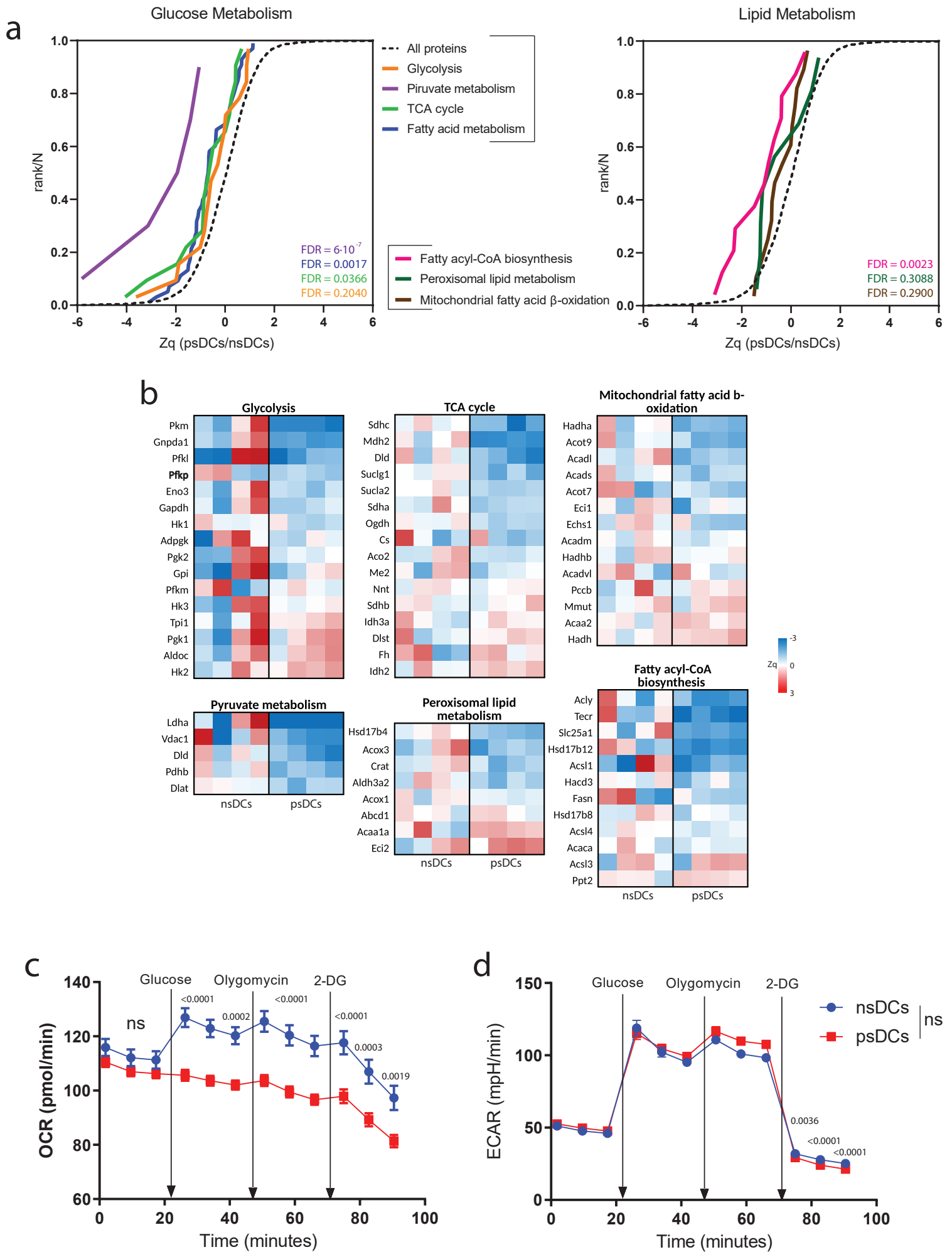
Figure S1



SUPPLEMENTARY FIGURE LEGENDS

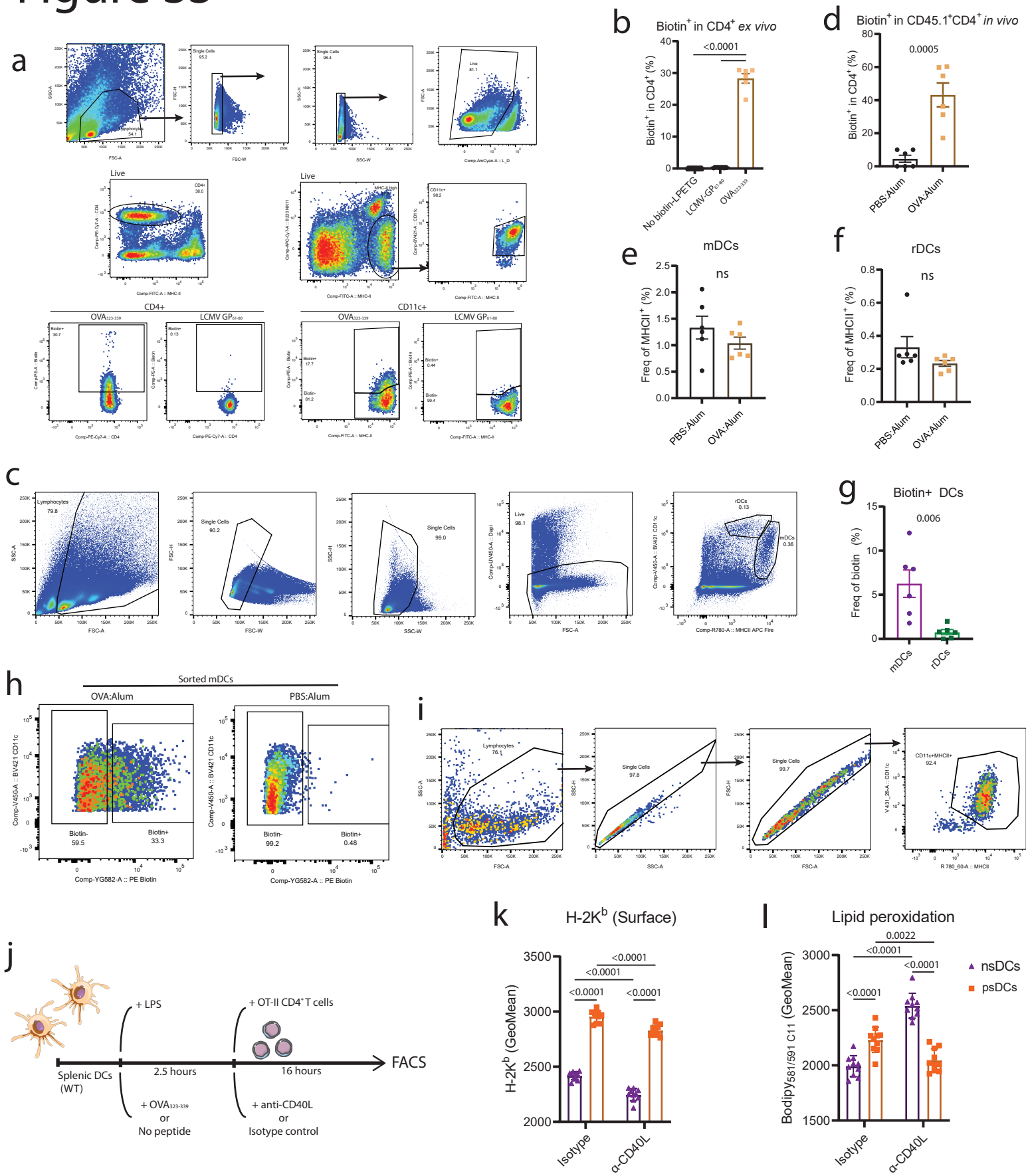
Supplementary Figure 1. Dynamic changes in protein expression in psDCs vs. nsDCs. Related to Figure 1. (a) Left, a confocal fluorescence maximal projection image of LPS-activated BMDCs in coculture with T cells. BMDCs were pre-loaded (psDCs) or not (nsDCs) with OVA₃₂₃₋₃₃₉ peptide and conjugated with T cells for 3 h in glass-bottom chambers pre-coated with fibronectin. Cells were then fixed and processed for immunofluorescence. Magenta, F-actin (phalloidin); green, α -Tubulin; red, DAPI. Bar, 10 μ m. Right, single confocal planes corresponding to the BMDC-T cell contact plane from the conjugates showed in the merge image. Single fluorescence channels for F-actin and α -tubulin are showed in grey-scale images. The centrosome is marked with a white arrow. (b) Partial least squares discriminant analysis (PLS-DA) of the psDC and nsDC biological replicates showing clustering of psDC samples performed with MetaboAnalyst 5.0. (c-f) Cumulative distribution of the protein abundance changes (Zq) showing the coordination in the behavior of proteins belonging to the selected functional categories compared to all proteins quantified in the experiment. Heatmaps showing the relative abundance changes (Zq) in all the nsDC and psDC biological replicates respect to the average value of the nsDC samples. Categories include (c) proteins belonging to the *Eukaryotic* (40S and 60S subunits) and *mitochondrial* (39S and 28S subunits) *ribosomes* or; (d) *Chromatin organization*, comparing histones and histone-interacting proteins; (e) the *ERAD pathway* related proteins; and (f) proteins belonging to the *Proteasome subunits* (11S, 19S, 20S and 20S core inducible proteins subunits).

Figure S2



Supplementary Figure 2. Coordinated protein changes reflect a change in metabolism in psDCs vs. nsDCs. Related to Figure 3. (a) Cumulative distribution of the protein abundance changes (Zq) corresponding to categories related to glucose (*Glycolysis*, *Pyruvate metabolism*, and *TCA cycle*; left) and lipid (*Fatty acyl-CoA biosynthesis*; *Peroxisomal lipid metabolism*, and *Mitochondrial fatty acid beta-oxidation*; right) metabolism. (b) Heatmaps showing the relative abundance changes (Zq) in all the nsDC and psDC biological replicates of the proteins belonging to the categories represented in A. (c) Mitochondrial respiration and (d) glycolytic activity obtained by Seahorse extracellular flux analysis of psDCs and nsDC during a glycolysis inhibition assay. For c-d $n = 8$ biological replicates with technical quintuplicates for each measure. Color code for c as in d. Data were analyzed in c and d using a two-way ANOVA. p-values are indicated, with ns for $p\text{-value} > 0.05$. 2-DG: 2-Deoxy-D-glucose.

Figure S3

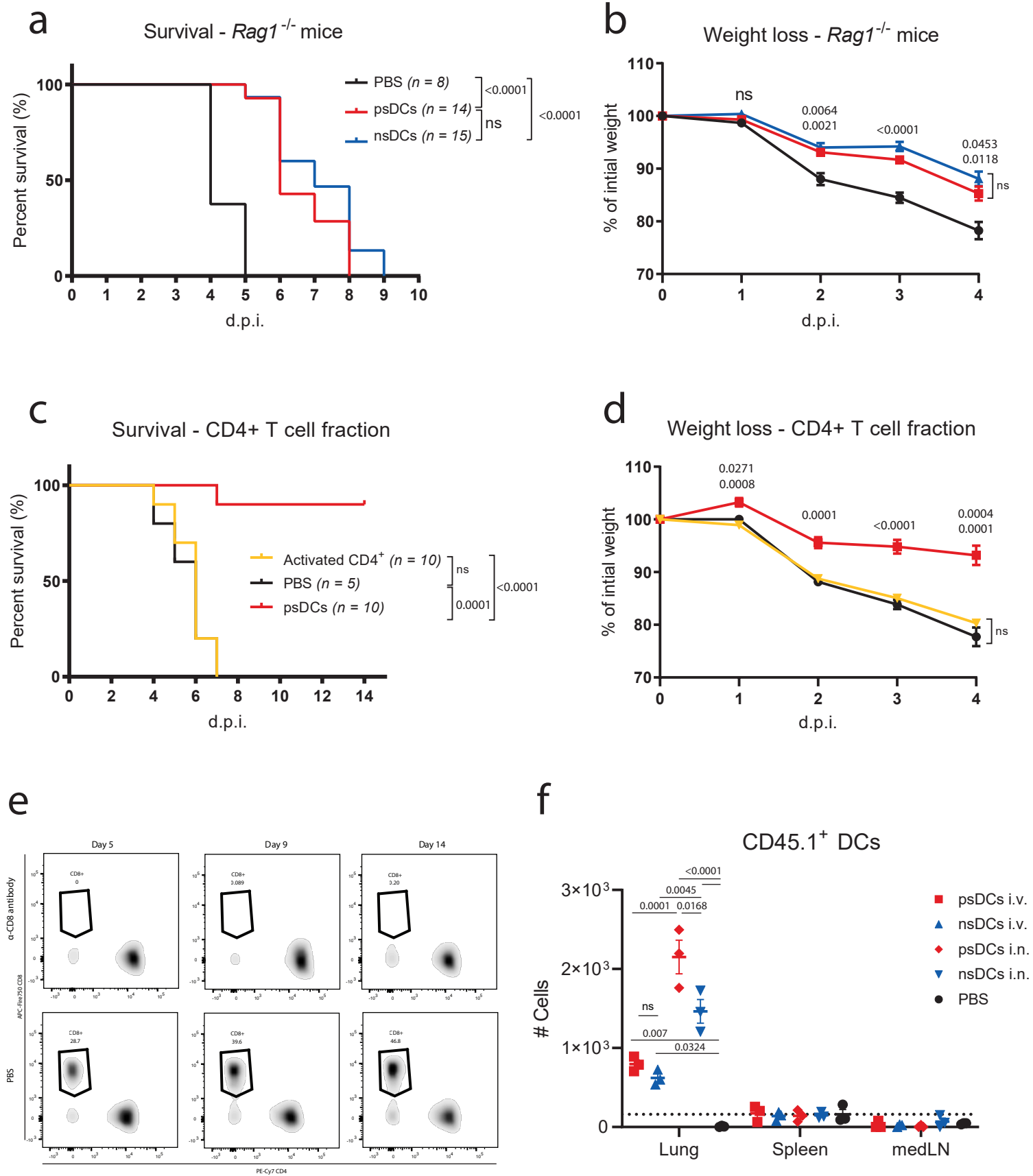


Supplementary Figure 3. Identification and analysis of biotin⁺ populations in LIPSTIC experiments. Related to Figure 4. (a) FACS gating strategy for the *ex vivo* LIPSTIC experiment shown in Figure 3B-C. (b) Flow cytometry analysis of biotin⁺ CD4⁺ T cells in CD4⁺CD45.1⁺ cells (*Cd40lg^{SrtA}*) after coculture with DCs pulsed with the indicated peptide (LCMV GP₆₁₋₈₀ or OVA₃₂₃₋₃₃₉). No biotin-LPETG indicates pulsing with OVA₃₂₃₋₃₃₉ but no addition of biotin-LPETG to the coculture. (c) Flow cytometry gating strategy used to identify mDCs in draining pLNs from immunized footpads in *in vivo* LIPSTIC experiments. (d) Flow cytometry analysis of biotin⁺ CD4⁺ T cells in CD4⁺CD45.1⁺ cells (*Cd40lg^{SrtA}*) extracted from popliteal lymph nodes (pLNs) from draining footpads immunized with the indicated formulation. FACS analysis of the proportions of (e) mDCs or (f) rDCs among live cells in pLNs of mice immunized with the indicated formulation. (g) Flow cytometry analysis of the proportions of biotin⁺ cells within the indicated population of DCs. (g) FACS analysis of the frequency of biotin⁺ mDCs in draining pLNs immunized with the indicated formulation. (g) Flow cytometry gating strategy to analyze the lipid peroxidation in sorted biotin⁺ or biotin⁻ mDCs shown in Figure 3H. (h) Sorting strategy to separate biotin⁺ and biotin⁻ within mDCs identified as in C. (i) Flow cytometry gating strategy for cells sorted as in H and stained with BODIPYTM 581/591 C11 for assessing lipid peroxidation in the CD11c⁺MHCII⁺ population. (j) *Ex vivo* experimental setup for K-L. Flow cytometry analysis of the geometric mean (GeoMean) of (k) H-2K^b or (l) lipid peroxidation in splenic DCs pulsed with OVA₃₂₃₋₃₃₉ (psDCs) or no peptide (nsDCs) generated in the presence of an anti-CD40L antibody or an isotype control. Data is representative of at least two independent experiments. For (b) and (d-g) *n* = 6. For (k-l) *n* = 10. Replicates are biological. Color code for (k) as in (l). Bar plots indicate mean ± SEM. Statistical significances are calculated with one-way ANOVA (b) or unpaired t-tests (d-g). p-values are indicated,

Calzada-Fraile D. et al.

with ns for $p\text{-value} > 0.05$. mDCs: migratory DCs. rDCs: resident DCs. pLNs: popliteal lymph nodes.

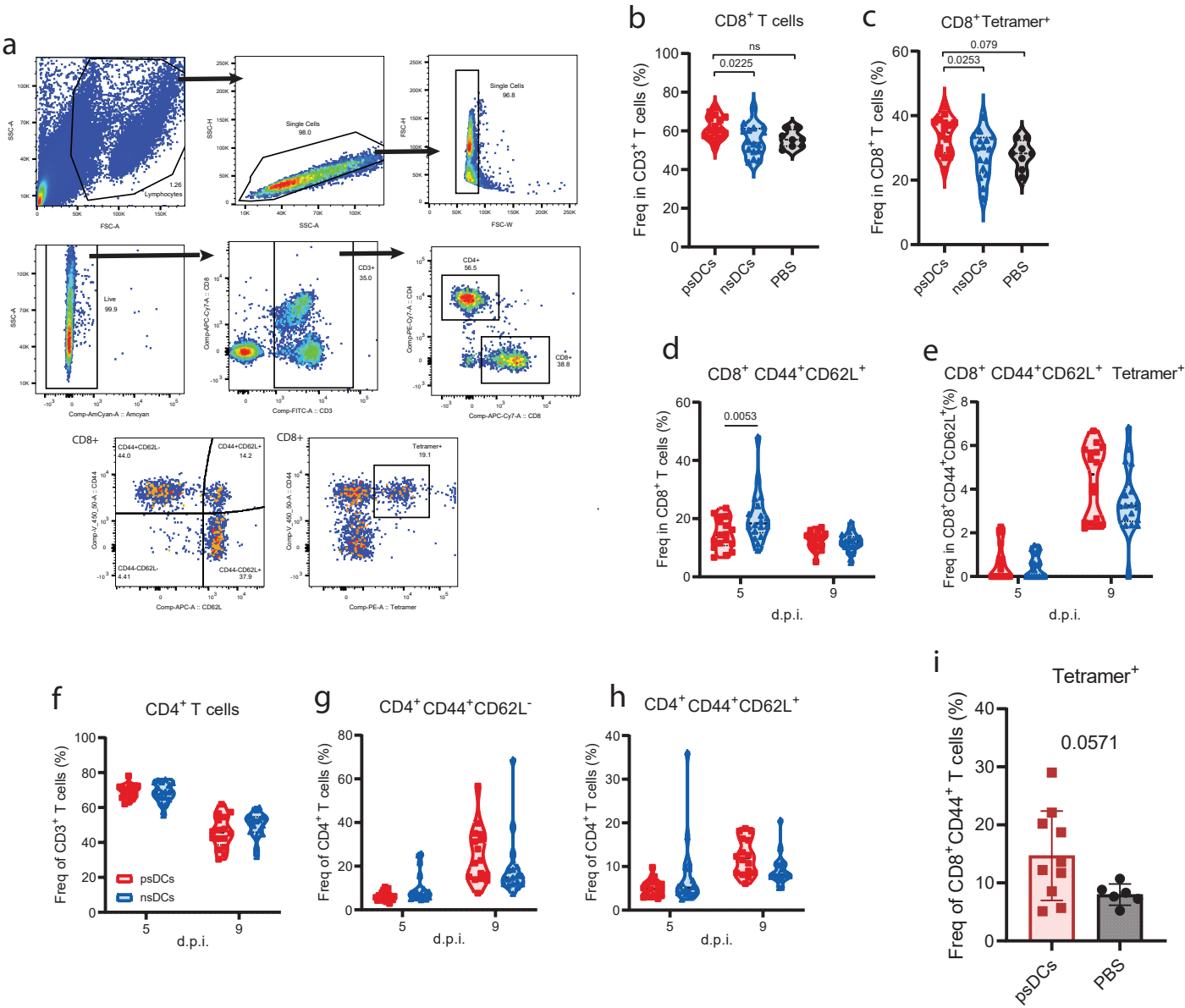
Figure S4



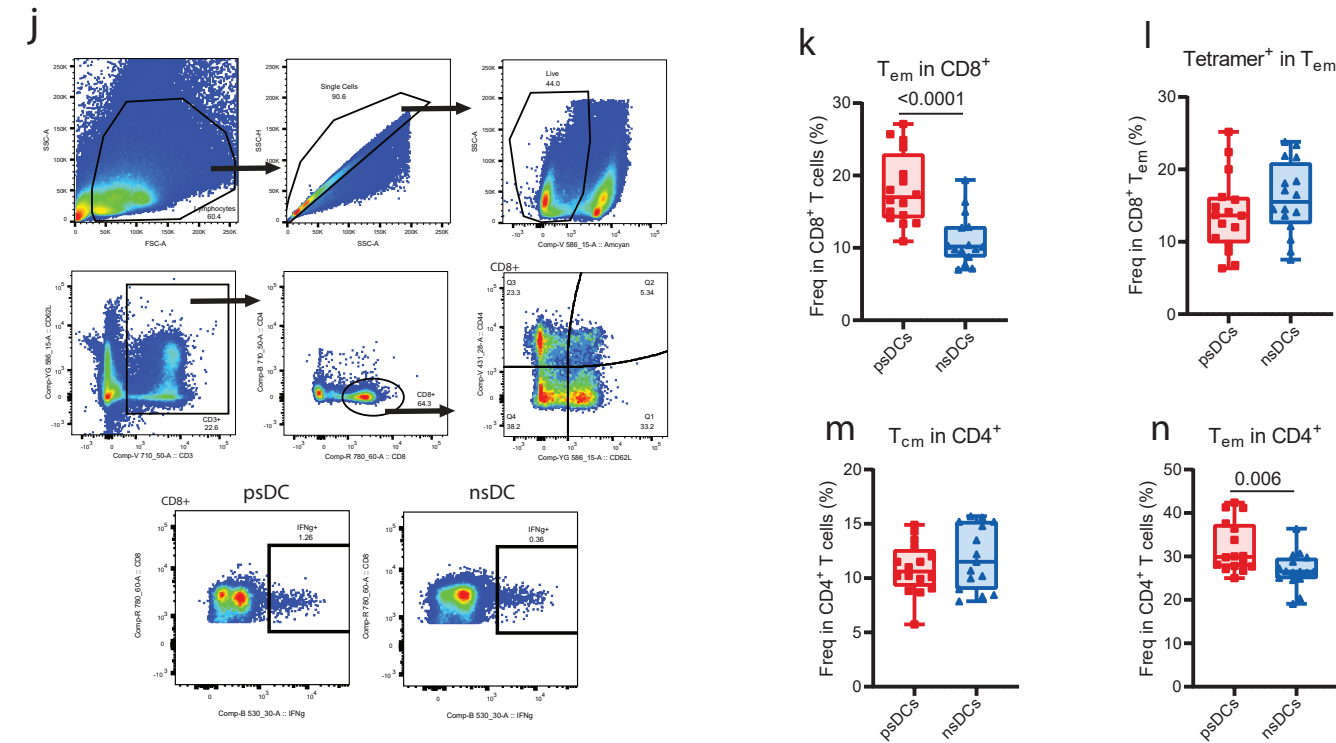
Supplementary Figure 4. Controls of *Listeria monocytogenes* infection upon transfer of psDCs. Related to Figure 5. (a) Survival and (b) weight loss of *Rag1*^{-/-} mice transferred with psDCs, nsDCs or PBS and then infected with a lethal dose of *Listeria monocytogenes*. Data are a pool of two independent experiments. For (b), *n* and color code as in (a). (c) Survival curves and (d) weight loss of mice that had been transferred $1 \cdot 10^6$ psDCs, $5 \cdot 10^4$ activated CD4⁺ T cells purified from the psDC coculture or PBS. Data are a pool of two independent experiments. For (d), *n* and color code as in (c). (e) Proportions of CD8⁺ T cells in the CD3⁺ T cell population upon a single intraperitoneal inoculation of 50 µg of a depleting anti-CD8 antibody or PBS at 5, 9 or 14 days after inoculation. (f) Number of CD45.1⁺ DCs (gated as CD45.1+CFSE+CD11c+) retrieved from the indicated organs 24 h after injection in CD45.2⁺ WT mice (*n* = 3). The dot line indicated the limit of detection due to electronic noise of the FACS calculated as the mean of PBS values in the spleen samples. Replicates are biological (mice). In (a-d), statistical analysis of survival curves was performed with the Gehan-Breslow-Wilcoxon test. Weights were compared using a mixed-effect model with the Geisser-Greenhouse correction and Tukey's multiple comparison test. In (f) statistical analysis is an unpaired one-way ANOVA performed for each organ dataset. *p*-values are indicated, with ns for *p*-value > 0.05. D.p.i.: days post-infection.

Figure S5

Acute



Memory

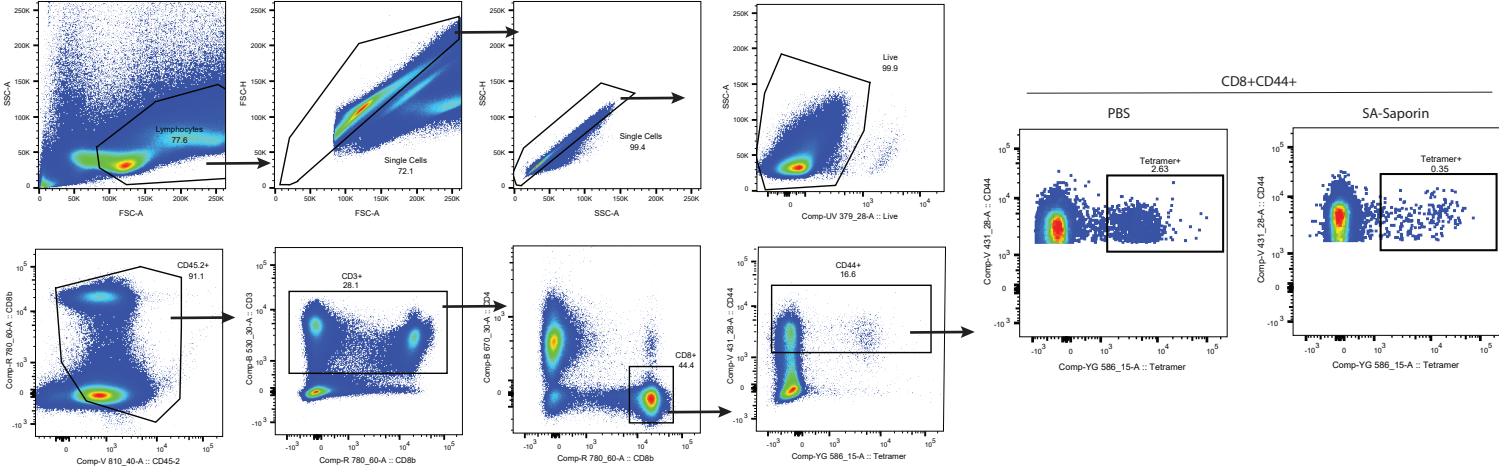


Supplementary Figure 5. Changes in other pathogen-specific acute and memory CD8⁺ T cell populations upon influenza virus infection after transfer of psDCs.

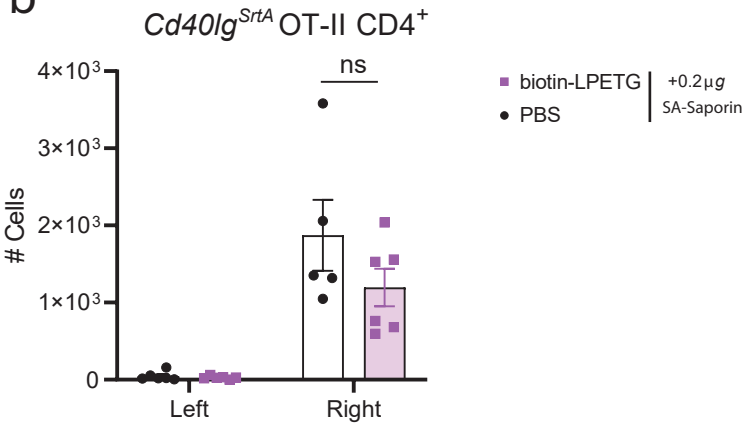
Related to Figure 6. (a) FACS gating strategy for peripheral blood cells. FACS analysis in peripheral blood at 9 after infection with an X31 influenza virus 24 h after injection of psDCs, nsDCs or PBS showing the frequency of (b) CD8⁺ T cells within CD3⁺ T cells, (c) tetramer⁺ cells within CD8⁺ T cells. FACS analysis in peripheral blood during acute infection at day 5 and 9 after infection showing: (d) the frequency of CD44⁺CD62L⁺ cells within CD8⁺ T cells, (e) the frequency of tetramer⁺ cells within CD44⁺CD62L⁺ CD8⁺ T cells, (f) proportion of CD4⁺ within T cells, (g) frequency of CD44⁺CD62L⁻ within CD4⁺ T cells, and (h) frequency of CD44⁺CD62L⁺ within CD4⁺ T cells. Color code for d-h indicated in f. (i) Frequency of tetramer⁺ cells within CD8⁺CD44⁺ T cells in peripheral blood 9 days after infection of Batf3^{-/-} mice that had been transferred with 5·10⁵ psDCs or the same volume of PBS. (j) FACS gating strategy for splenocytes. FACS analysis in spleen of mice during the memory phase day 30 after infection showing: (k) the frequency of Tem (CD44⁺CD62L⁻) within CD8⁺ T cells, (l) proportions of tetramer⁺ cells within Tem CD8⁺ T cells, (m) frequency of Tem within CD4⁺ T cells, and (n) frequency of Tem within CD4⁺ T cells. All data are representative two independent experiments. For (b-c) $n = 16$ for psDC and nsDC and $n = 8$ for PBS, while for (d-h) $n = 18$ for nsDC and $n = 17$ at day 5 and $n = 16$ at day 9 for psDC. For (k) and (m) $n = 16$ for psDC and $n = 15$ for nsDC, while for (l) and (n) $n = 16$. For (i) $n = 10$ for psDC and $n = 6$ for PBS. Replicates are biological (mice). Statistical analyses are result of one-way ANOVA (b-c), a mixed-effect model with and Sidák's multiple comparison test (d-h) or unpaired t-test (i and k-n). MFI: mean fluorescence intensity. p-values are indicated, with ns for $p\text{-value} > 0.05$. D.p.i.: days post-infection.

Figure S6

a



b



Supplementary Figure 6. Identification of SIINFEKL-specific CD8⁺ T cell upon immunization. Related to Figure 7. (a) Flow cytometry gating strategy of popliteal lymph nodes identifying SIINFEKL-specific CD8⁺ T cells upon pSDC depletion shown in Figure 6. (b) Counts of CD40L-SrtA OT-II CD4⁺ T cells (gated as CD45.1⁺CD4⁺ T cells) in draining popliteal lymph nodes from the immunized (right) or contralateral (left) side 8 days after immunization. The counts represent the cells contained in one full pLN. Data are representative of two independent experiments. $N = 6$ animals. Bar plots indicate mean \pm SEM. Statistical tests are unpaired two-way ANOVA. Data is representative two independent experiments. For ns, $p\text{-value} > 0.05$.